Grazing-Incidence X-Ray Diffraction

Sergey Stepanov

Illinios Institute of Technology, BioCAT at the Advanced Photon Source,

Argonne National Lab, 9700 S. Cass Ave., Bldg.435, Argonne, IL 60439

Contents

1. Geometry of GID
2. Typical applications
3. Experimental setups
4. Kinematical vs dynamical theory
5. GID in multilayers and matrix dynamical theory
6. Diffuse scattering in GID

1. Geometry of GID

Grazing-incidence diffraction is a scattering geometry combining the Bragg condition with the conditions for x-ray total external reflection from crystal surfaces. This provides superior characteristics of GID as compared to the other diffraction schemes in the studies of thin surface layers, since the penetration depth of x-rays inside the slab is reduced by three orders of magnitude (Fig.1) -- typically from 1-10μm to 1-10nm (10-100Å).

The geometry of GID can be approached by two different ways.

1. Let we have a setup for usual x-ray reflectivity (Fig.2a). The wave E_0 incident on the surface at a small angle Φ_0 produces specularly reflected wave E_s. Now, let us rotate the sample round its surface normal, thus preserving the small angle Φ_0. At this rotation, the wave E_0 can make the Bragg angle Θ_B with some atomic planes perpendicular to the surface and originate the diffracted wave. This diffracted wave will be directed at a small angle inwards the sample, because there is no momentum transfer pushing it outwards (the reciprocal lattice vector is parallel to the surface). However, in spite of the generation inside crystal, it occurs that the diffracted wave can experience the same specular reflection effect as for the incidence wave. This gives rise to specular diffracted wave E_h that takes off the crystal at a small angle Φ_h. The value of Φ_h can differ from Φ_0, but we shall discuss it later. One can also

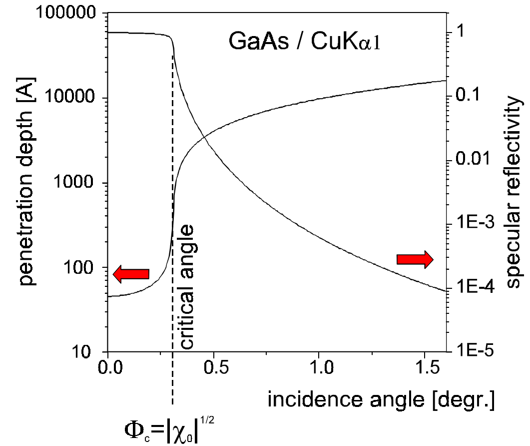

Fig.1 Penetration depth and reflectivity of x-rays at grazing angles

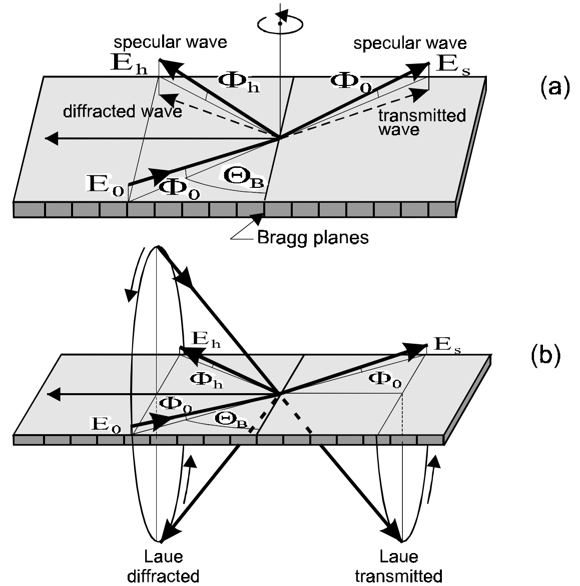

Fig.2 Geometry of GID

consider that the wave E_h is generated by the Bragg diffraction of specularly reflected wave E_s. Both the presentations are simplified because in reality the processes of Bragg diffraction and specular reflection interact with each other and cannot be separated out. The most important fact is that E_h principally contains information on the structure of very thin surface layer.

2. GID can be also be viewed as a specific case of symmetric Laue diffraction (Fig.2b). When sample set in the conditions for Laue diffraction is rotated by 90º round the reciprocal lattice vector, the Bragg angle is preserved and we end up with GID. This approach is often helpful for understanding some effects in GID. For example, like in usual Laue diffraction, in GID there are Borrmann and anti-Borrmann wavefields with weaker and stronger interaction with crystal, respectively.

Let us discuss the angles where GID is characterized by the maximum sensitivity to thin layers. The intuitive estimate is that either Φ_0 or Φ_h should be less than the critical angle $\Phi_c = |\chi_0|^{1/2}$ for total external reflection (Fig.1). Then, either the illuminated depth should be as small as a few nanometers, or the diffracted intensity would yield from this small depth. Such an estimate is correct for kinematic GID from highly disordered crystals. For dynamical GID the total reflection conditions differ for the Borrmann and anti-Borrmann fields (Fig.3). The anti-Borrmann field behaves more or less as expected – either Φ_0 or Φ_h should be small; while the Borrmann field is totally reflected only when both of the angles are small. That means, e.g., that you can illuminate a crystal at a small angle and see the GID signal from relatively deep layers.

Before proceeding to applications we need to introduce one more effect specific to GID. The conditions: $\mathbf{k}_h^2 = \mathbf{k}_0^2$ and $\mathbf{k}_{h\perp} = \mathbf{k}_{0\perp} + \mathbf{h}_\perp$ allow to determine $\mathbf{k}_{hz}$ and the angle Φ_h :

$$\Phi_h^2 = \Phi_{hB}^2 - \alpha \quad , \qquad (1)$$

where $\Phi_{hB} = |\Phi_0 + h_z/k_0|$ and $\alpha = (2\mathbf{k}_0\mathbf{h}+\mathbf{h}^2)/\mathbf{k}_0^2 = -2\sin\Theta_B\ (\Theta-\Theta_B)$. Eq.(1) has an interesting consequence: since the angles Φ_0 and Φ_h have the order of 1mrad, the deviations of incidence wave from Bragg angle by a few seconds of arc are resulted in 1000 times greater changes of Φ_h (see Fig.4). This effect is widely used for the measurements of GID.

Finally, GID is not the only geometry combining Bragg diffraction and total external reflection. Other grazing geometries are extremely asymmetric (EAD) diffraction with either grazing incidence or grazing exit (Fig.5a) and grazing Bragg-Laue (GBL) diffraction (Fig.5b). EAD is realized when the Bragg angle coincides with the misorientation angle φ of the Bragg planes. With few exceptions this requires tunable x-ray source (synchrotron). The advantage is the possibility to measure both the normal and lateral strains and have surface sensitivity comparable with that of GID. The Bragg-Laue scheme is similar to GID, but the diffracted wave is pushed out of crystal due to a small miscut of atomic planes (1-5°) instead of the specular reflection effect. This provides some more freedom in selecting the incidence angle than in GID. The surface sensitivity is slightly less, but

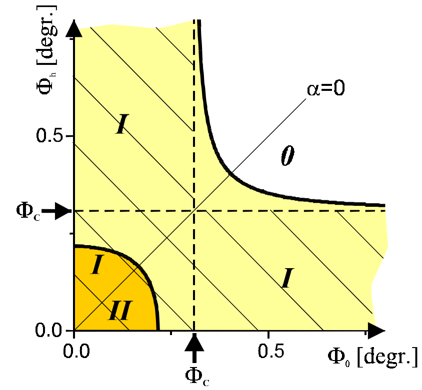

Fig.3. Angular area of total reflection for anti-Borrmann (*I*) and Borrmann (*II*) x-ray fields. The total reflection area for kinematical GID is hatched.

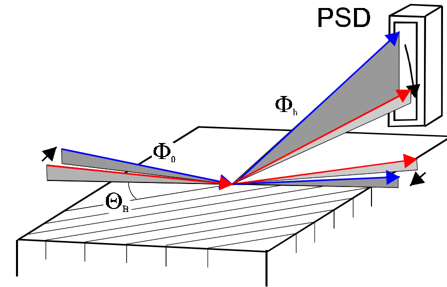

Fig.4. Dependence of diffracted wave takeoff on the deviation from Bragg condition in GID.

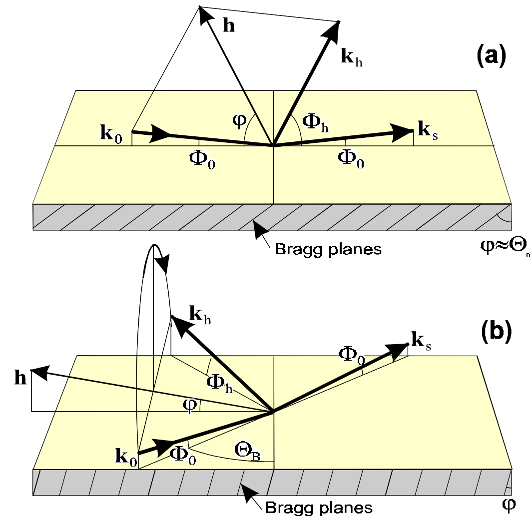

Fig.5. Geometries of (a):extremely asymmetric diffraction (grazing-incidence case) and (b): grazing Bragg-Laue diffraction.

the experimental implementation is much easier. The great scheme for laboratory use!

2. Typical applications

The major application of GID is to measure strain relaxation in thin layers and multilayers (see Fig.6 and Refs.[10,16,18,19]). Here are two advantages of GID as compared with usual symmetric Bragg-case diffraction. First, as we have discussed, x-ray extinction in GID is reduced by several orders magnitude, i.e. much thinner layers become

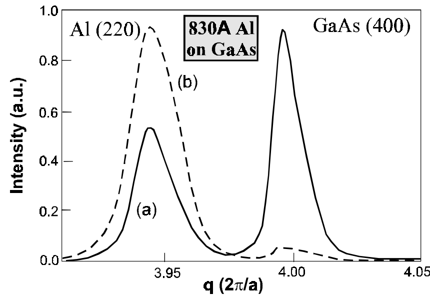

Fig.6. The first application of GID to studies of relaxation in thin epitaxial layers [9]. (a): GID curve at Φ_0 corresponding to x-ray total reflection at the GaAs substrate. (b): The enhancement in signal at a smaller angle when total reflection occurs at the Al overlayer surface.

accessible. Moreover, the extinction of GID can be varied changing the incidence angle (i.e. the probed depth can be tuned in order to meet sample requirements). Second, GID measures lattice relaxation directly (the scattering is from atomic planes perpendicular to the surface), while in the Bragg case it is measured indirectly (through the change in normal lattice spacing).

At present, practically all the other techniques developed for usual Bragg diffraction have been implemented in GID too. This allowed adapting the requirements of modern microelectronics research by extending x-ray diffraction techniques to much thinner layers. For example, one can study point defects in thin layers with Huang diffuse scattering in GID [15]. Even the methods of x-ray structure analysis have been transferred to GID and applied with success to surface crystallography problems (especially to the studies of surface reconstruction).

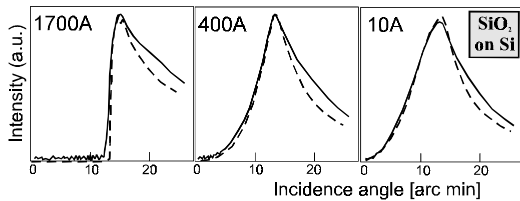

Fig.7. Detection of thin amorphous films on crystal surfaces with the help of GID [10].

Unfortunately, this interesting topic is outside the scope of our discussion.

On the other hand, a series of GID applications uses the approaches developed in x-ray reflectometry. For example, one can measure the thickness of amorphous surface layer recording the integral intensity of GID as a function of the incidence angle (i.e. like in usual x-ray specular reflectivity measurements, but with x-ray detector in the diffracted beam direction). Since amorphous films attenuate x-ray intensity incident onto the crystal and at small angles the attenuation is stronger, then, the thicker is the film, the greater is the reduction of GID reflectivity at small angles (Fig.7). Such a technique turned our to be very effective for the measurements of amorphization effects in ion implantation [11,12,17]. Another example of this kind is the application of GID to the studies of surface and interface roughness. The sensitivity of GID to roughness is equivalent to that of x-ray specular reflection experiments. This is because the angles with the surface are of the same order. However, it turns out that GID can provide a unique information on atomic ordering inside roughness [20].

3. Experimental Setups

Now, when you are familiar with *what* is possible to measure with GID, let us discuss *how* to measure it. The major types of GID schemes are presented on Fig.8.

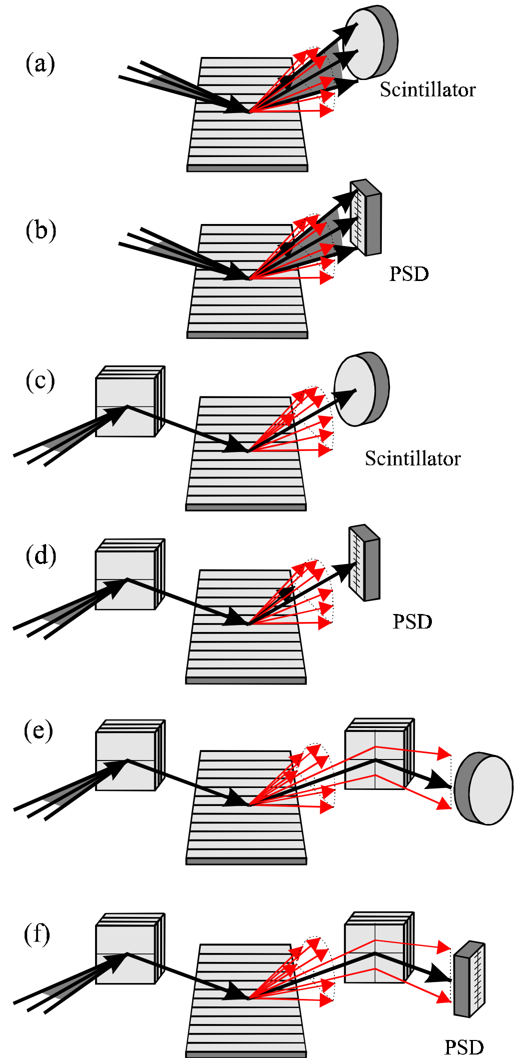

Fig.8. Different schemes of measurements in GID. (a): integral reflectivity, (b,c): "double-crystal" (coherent + diffuse scattering alltogether). (d,e): "triple-crystal" (2D mapping of DS). (f): 3D mapping of DS.

With the scheme (a) you can measure the integral reflectivity of GID as a function of the incident angle (like the curves on Fig.7). This is the simplest scheme easily implemented in laboratory

environment with ordinary x-ray tubes. It is good for the detection of amorphous layers. However, this is, probably, the only possible application.

The schemes (b) and (c) present two possible types of "double-crystal" measurements in GID. The difference between (c) and corresponding usual schemes is the necessity of the second angular collimation of incidence beam (over the grazing angle) and a very strong spatial collimation (in order to avoid great footprint of the grazing beam and scattering from crystal edges). This is normally not achievable in laboratory. The scheme (b) is often equivalent to (c) because of Eq.(1), as illustrated on Fig.4. When implemented with a position sensitive detector (PSD), this scheme provides much better intensity conditions (the beam is not collimated over the Bragg angle), which principally can be met in laboratory. However, this scheme is not applicable to the measurements of strain relaxation: in the presence of relaxation Eq.(1) can be roughly applied to the Bragg angle of each lattice spacing in crystal and the relation between Φ_h and $(\Theta-\Theta_B)$ becomes meshed.

Schemes (d), (e), and (f) are for separating out coherent GID reflection and diffuse scattering (DS) from defects. These normally require synchrotron radiation. Among (d) and (e), the former one is easier in use, since no analyzer adjustment is necessary with respect to diffracted beam with strong vertical spread. The complete solution to the problem of DS measurements is only given by the scheme (f), which corresponds to three-dimensional mapping of reciprocal space. A more detailed discussion on high-resolution measurements in GID can be found in [5].

Kinematical vs dynamical theory

Like the x-ray diffraction in other geometries, GID can be described with either kinematical or dynamical theory. As known, the kinematical theory is a perturbation theory treating diffraction as a single scattering event with negligible effect on the intensity of initial waves. According to this theory, the scattering amplitude E_h is given by the matrix element of the perturbation $\chi(z)=\chi_h(z)\exp[ih_z(z)z]$ with the two wavefields which are produced in target by the incident wave E_0 and the inverted diffracted wave E^{out}. The latter one is the wave illuminating the crystal from the place where is your detector (see Fig.9a):

$$E_h \sim \int D^{out}(z)\chi(z)\, D^{in}(z)dz \quad , \qquad (2)$$

In conventional diffraction geometries it is common to neglect the refraction and specular reflection effects of x-rays. Then, both the initial waves are plane: $D^{in}(z)=E_0\exp(ik\Phi_0 z)$, $D^{out}(z)=E^{out}\exp(ik\Phi_h z)$. This gives the well-known Born approximation (comp. Fig.9b).

In GID, the waves the specular reflection is essential

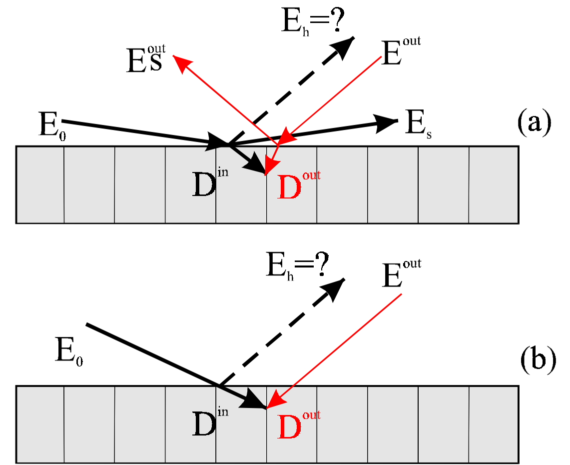

Fig.9. On the kinematical theory for (a): GID and (b): usual diffraction.

and D^{in}, D^{out} are given by the Fresnel equations. For example, for a perfect crystal: $D^{in} = (\Phi_0-u_0)/(\Phi_0+u_0)\exp(iku_0z)$, $D^{out} = (\Phi_h-u_h)/(\Phi_h+u_h)\exp(iku_hz)$, where $u=(\Phi^2+c_0)^{1/2}$. For a

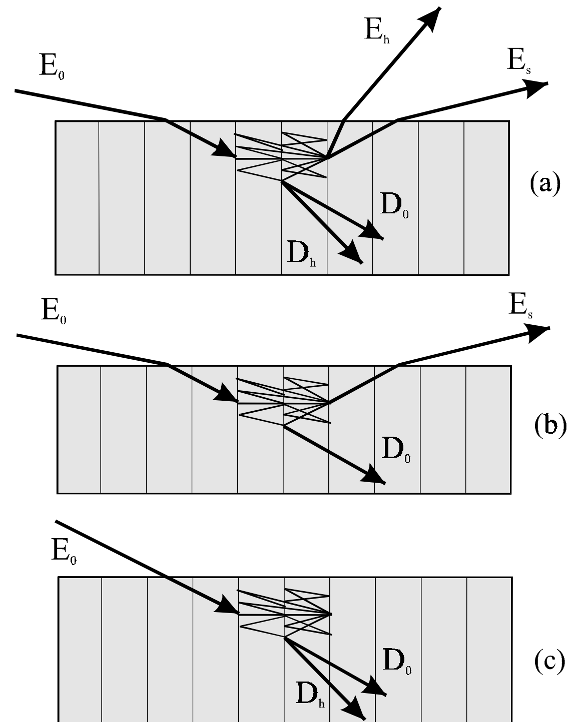

Fig.10. On the dynamical theory for (a): GID, (b): specular reflection, and (c): Laue-diffraction.

multilayer, these wave fields are given by Parratt's or Abeles method as a solution to respective x-ray specular reflection problem [31,32]. The solution must be obtained twice -- for E_0 and E^{out} incident waves.

If your crystal is perfect, you have to consider the interpretation of your data with the dynamical theory. In the 70s, at the beginning of GID studies there were some doubts whether GID needs a

dynamical theory at all. The argument put forward, e.g. by Vineyard [30] was, that the penetration of x-rays in crystals is very small and therefore any multiple scattering effects are negligible. However, numerous posterior experiments (see, for example, [1,3,4]) proved the existence of multiple dynamical effects in GID. The necessity of the dynamical theory is stimulated by permanently improving quality of semiconductor structures, which are the main object of GID applications.

Multiple scattering effects are essential in GID because the Bragg planes are perpendicular to the surface, so therefore x-rays are multiply scattered *along* the surface (Fig.10a). Clearly, the theory has to take into account x-ray refraction and specular reflection at the surface (and internal interfaces, if present). This provides two differences with conventional cases:

(a) The terms (k_0^2-k^2) and (k_h^2-k^2) in the dispersion equation cannot be approximated as $2k(k_0-k)$ and $2k(k_h-k)$, respectively. It means, that the dispersion equation is the fourth-order polynomial providing four pairs of transmitted and diffracted waves: $D_h^{(j)}=v^{(j)}D_0^{(j)}$, j=1,2,3,4. Among these fields, one is the Borrmann field, one is anti-Borrmann field, and the other two are specularly reflected Borrmann and anti-Borrmann fields respectively.

(b) The boundary conditions are formulated for x-ray waves and their derivatives and contain the specular waves. For a perfect crystal without any layers these are (see Fig.10a):

$$E_0 + E_s = D_0^{(1)} + D_0^{(2)} , \quad (3)$$

$$\Phi_0 E_0 - \Phi_0 E_s = u^{(1)}D_0^{(1)} + u^{(2)}D_0^{(2)} , \quad (4)$$

$$E_h = v^{(1)}D_0^{(1)} + v^{(2)}D_0^{(2)} , \quad (5)$$

$$-\Phi_h E_h = w^{(1)}D_0^{(1)} + w^{(2)}D_0^{(2)} . \quad (6)$$

Here $u^{(j)}=k_{0z}^{(j)}/k$ are the solutions to the dispersion equation and $w^{(j)}=v^{(j)}(u^{(j)}+h_z/k)$. Eqs.(3)-(4) contain the fields j=1,2 only, because the fields j=3,4 have zero amplitudes (there are no specular waves inside thick substrates, because there is no lower interface to originate them).

Now, let us compare these equations with those for conventional x-ray specular reflection (Fig.10b):

$$E_0 + E_s = D_0 ,$$
$$\Phi_0 E_0 - \Phi_0 E_s = uD_0 ,$$

and with those for conventional Laue-case diffraction (Fig.10c):

$$E_0 = D_0^{(1)} + D_0^{(2)} ,$$
$$0 = v^{(1)}D_0^{(1)} + v^{(2)}D_0^{(2)} .$$

You can see that all the structure of equations in all the three cases is similar. That gives some drive to obtain a universal algorithm for the calculations of GID, usual diffraction and specular reflection.

5. GID in multilayers and matrix dynamical theory

The dynamical theory outlined in the previous section is for perfect crystals without defects. Let us discuss how can it be extended for strained crystals and multilayers. A serious theoretical problem is that usual Takagi-Taupin approach is not applicable: the x-ray wave fields vary with depth at nearly interatomic scale, so that their second derivatives cannot be neglected. One has to apply either matrix extension of the Takagi equations [38,39], or try to construct something like Abeles' matrix method or Parratt's recursion equations known for x-ray specular reflection from multilayers.

An analog of Abeles method for GID can be derived in a straightforward way [16,41,42]. Let we have a multilayer, or a crystal formally subdivided into a series of layers with invariable crystal structure within each layer. Then, the dynamical diffraction equations for a perfect crystal can be applied for each layer and the boundary conditions like (3)-(6) can be put at each interface. The latter can be presented in a (4x4) matrix form for vectors $D_n=(D_{0n}^{(1)}, D_{0n}^{(2)}, D_{0n}^{(3)}, D_{0n}^{(4)})$:

$$E=S_1D_1 , \quad D_1=S_2D_2 , \ldots\ldots D_{N-1}=S_ND_N ,$$

or

$$E=SD_N . \quad (7)$$

Here S are the (4x4) matrices composed by $v_n^{(j)}$, $u_n^{(j)}$, $w_n^{(j)}$, etc; $S= S_1 S_{2\ldots\ldots} S_n$, and $E=(E_0,0,E_s,E_h)$.

Eq.(7) formally solves the problem, because it contains four simple linear equations for four unknown amplitudes (E_s, E_h, $D_{0N}^{(1)}$, $D_{0N}^{(2)}$). However, it provide divergences for thick multilayers. There are some workarounds on this problem with the help of dynamically varied thick crystal approximation (see e.g. [42]). However, in the range where the anti-Borrmann x-ray field is reflected and the other one not, the problem becomes inevitable.

A complete solution to the problem has been obtained with further development of the same matrix method and proceeding to recursive equations for (2x2) blocks of original (4x4) matrices. The new approach, yet unpublished, has been tested with GID and EAD from GaAs/AlAs multilayers and proven to work perfectly. Far from the Bragg angle it reduces to scalar recursive equations by Parratt, and far from grazing incidence and exit it gives the recursive equations by Bartels, Honstra and Loobeck for multilayer diffraction.

At present I am developing a WWW interface to the program based on this algorithm and simulating multilayer diffraction in GID, EAD and GBL. The interface should be ready at the beginning of November. For those, who are interested, please, check the link:

http://sergey.bio.aps.anl.gov

I will report there on my advances with this project.

6. Diffuse scattering in GID

As soon as the diffraction problem for multilayer is solved, the obtained fields can be used for the calculation of scattering from point-like defects, dislocation loops, roughness, etc. If I stay in time, I am going to give here an example of such calculations -- a study of roughness effects on GID. Alternatively, I suggest having a look at Ref.[19].

References

GID general:

[1] A.L.Golovin, R.M.Imamov, and S.A.Stepanov. Experimental study of x-ray diffraction under specular reflection conditions. *Acta Cryst.A*, 40:225, 1984.

[2] H.Dosch, B.W.Batterman, and D.C.Wack.Depth-controlled grazing-incidence diffraction of synchrotron x-radiation. *PRL*, 56:1144, 1986.

[3] N.Bernhard, *et al*. Grazing incidence diffraction of x-rays at a Si single crystal surface: Comparison of theory and experiment. *Z.Phys.B*, 69:303, 1987.

[4] T.Jach, P.L.Cowan, Q.Shen, and M.J.Bedzyk. Dynamical diffraction of x-rays at grazing angle. *PRB*, 39:5739, 1989.

[5] E.A.Kondrashkina, *et al*. High-resolution grazing-incidence x-ray diffraction for characterization of defects in crystal surface layers. *J.Appl.Phys*., 81(1):175--183, 1997.

EAD general:

[6] H.R.Hoche, J.Nieber, and O.Brummer. Extremely skew x-ray diffraction. *Acta Cryst. A*, 42:585, 1986.

[7] S.Kimura, J.Harada, and T.Ishikawa. Comparison between experimental and theoretical rocking curves in extremely asymmetric Bragg cases of x-ray diffraction. *Acta Cryst. A*, 50:337, 1994.

GBL general:

[8] P.A.Aleksandrov, A.M.Afanas'ev, and S.A.Stepanov. Bragg-Laue diffraction in inclined geometry. *Phys.Stat.Sol. A*, 86:143, 1984.

GID applications:

[9] W.C.Marra, P.Eisenberger, and A.Y.Cho. X-ray total-external-reflection Bragg diffraction: a structural study of the GaAs-Al interface. *J.Appl.Phys.*, 50:6927, 1979.

[10] A.L.Golovin and R.M.Imamov. Obtaining quantitative information on amorphous layer thickness on crystal surface using x-ray diffraction under specular reflection conditions. *Phys.Stat.Sol. A*, 80:K63, 1983.

[11] A.L.Golovin, R.M.Imamov, and E.A.Kondrashkina. Potentialities of new x-ray diffraction methods in structural studies of ion-implanted silicon layers. *Phys.Stat.Sol. A*, 88:505, 1985.

[12] R.M.Imamov, *et al*. Study of silicon surface layers implanted by heavy metals ions with the application of x-ray diffraction under total external reflection conditions. *Poverkhn., Fiz.Khim.Mekh.*, (3):41, 1987.

[13] A.Segmuller. Characterization of epitaxial films by grazing-incidence x-ray diffraction. *Thin Solid Films*, 154:33, 1987.

[14] H.Dosch, *et al*. Experimental evidence for an interface delocalization transition in Cu_3Au. *PRL*, 60:2382, 1988.

[15] S.Grotehans, *et al*. Diffuse scattering of x-rays at grazing angles from near-surface defects in crystals. *PRB*, 39:8540, 1989.

[16] A.A.Williams, *et al*. Strain relaxation during the initial stages of growth in Ge/Si(001). *PRB*, 43:5001, 1991.

[17] S.Rugel, G.Wallner, H.Metzger, and J.Peisl. Grazing-incidence x-ray diffraction on ion-implanted silicon. *J.Appl.Cryst.*, 26:34, 1993.

[18] U.Pietsch, *et al*. Depth-resolved measurement of lattice relaxation in Ga_{1-x}/In_x/As/GaAs strained layer superlattices by means of grazing-incidence x-ray diffraction. *J.Appl.Phys.*, 74:2381, 1993.

[19] V.H.Etgens, *et al*. ZnTe/GaAs(001): Growth mode and strain evolution during the early stages of molecular-beam-epitaxy heteroepitaxial growth. *PRB*, 47:10607, 1993.

[20] S.A.Stepanov, *et al*. Diffuse scattering from interface roughness in grazing incidence x-ray diffraction. *PRB*, 54:8150, 1996.

EAD applications:

[21] A.Fukuhara and Y.Takano. Asymmetric x-ray Bragg reflexion and shallow strain distribution in silicon single crystals. *J.Appl.Cryst.*, 10:287, 1977.

[22] B.K.Tanner and M.J.Hill. Double axis x-ray diffractometry at glancing angles. *J.Phys.D*, 19:L229, 1986.

[23] L.Tapfer and K.Ploog. Improved assessment of structural properties of $Al_xGa_{1-x}As$/GaAs heterostructures and superlattices by double-crystal x-ray diffraction. *PRB*, 33:5565, 1986; ibid: 40:9802 (1989).

[24] C.A.Lucas, *et al*. Characterization of nanometer-scale epitaxial structures by grazing-incidence x-ray-diffraction and specular eflectivity. *J.Appl.Phys.*, 63:1936, 1988.

[25] H.-G.Bruhl, *et al*. Extreme asymmetric x-ray Bragg reflection of semiconductor heterostructures near the edge of total external reflection. *J.Appl.Cryst.*, 23:228, 1990.

[26] L.Tapfer, *et al*. X-ray diffraction study of corrugated semiconductor surfaces, quantum wires and quantum boxes. *Appl.Surf.Sci.*, 60/61:517, 1992.

[27] S.Kimura, *et al*. Surface-selective x-ray topographic observations of mechanochemical polished silicon surfaces using synchrotron radiation. *Appl.Phys.Lett.*, 60:2604, 1992.

GBL applications:

[28] A.M.Afanas'ev, *et al*. Grazing Bragg-Laue diffraction for studying the crystal structure of thin films. *Phys.Stat.Sol. A*, 86:K1, 1984; ibid: 90:419 (1985).
[29] A.M.Afanas'ev, *et al*. Three-crystal x-ray spectra of crystals with disturbed surface layer in slipping Bragg-Laue geometry. *Kristallografiya*, 31:1066, 1986; [*Sov.Phys. -- Crystallogr.* 31:630, 1986].
[30] G.D.Yao, J.Wu, T.Fanning, and M.Dudley. Investigation of semiconductor heterostructures by white beam synchrotron x-ray topography in grazing Bragg-Laue and conventional geometries. *Adv. X-Ray Anal.*, 35:247, 1992.

Extended kinematical theory (DWBA):

[31] G.H.Vineyard. Grazing-incidence diffraction and the distorted-wave approximation for the study of surfaces. *PRB*, 26:4146, 1982.
[32] O.G.Melikyan and A.M.Meretukov. Kinematic grazing-incidence x-ray diffraction from a superlattice. *Kristallografiya*, 38:42, 1993 [*Crystallogr.Rep.* 38:311, 1993].
[33] G.T.Baumbach, S.Tixier, U.Pietsch, and V.Holy. Grazing-incidence diffraction from multilayers. *PRB*, 51:16848, 1995.

Extended dynamical theory:

[34] S.Kishino and K.Kohra. Theoretical considerations on Bragg-case diffraction of x-rays at a small glancing angle. *J.Appl.Phys.*, 10:551, 1971.
[35] T.Bedynska. On x-ray diffraction in an extremely asymmetric case. *Phys.Stat.Sol. A*, 19:365, 1973.
[36] J.Hartwig. On the integrated reflectivity of perfect crystals in extremely asymmetric Bragg cases on x-ray diffraction. *Acta Cryst. A*, 37:802, 1981.
[37] V.M.Kaganer, *et al*. Laue-to-Bragg transition in extremely asymmetric dynamic neutron diffraction. *Phys.Stat.Sol. A*, 71:371, 1982.
[38] A.M.Afanas'ev and M.K.Melkonyan. X-ray diffraction under specular reflection conditions. Ideal crystal. *Acta Cryst. A*, 39:207, 1983.
[39] M.A.Andreeva, K.Rocete, and Yu.P.Khapachev. Matrix analog of the Takagi equations for grazing-incidence diffraction. *Phys.Stat.Sol. A*, 88:455, 1985.
[40] D.W.Berreman and A.T.Macrander. Asymmetric x-ray diffraction by strained crystal wafers: 8x8-matrix dynamical theory. *PRB*, 37:6030, 1988.
[41] A.M.Afanas'ev and O.G.Melikyan. Modified theory (MDT) of x-ray diffraction in exteremely asymmetric schemes. *Phys.Stat.Sol. A*, 122:459, 1990.
[42] S.A.Stepanov and R.Koehler. A dynamical theory of extremely asymmetric x-ray diffraction taking account of normal lattice strain. *J.Phys.D*, 27:1923, 1994.
[43] S.A.Stepanov, U.Pietsch, and G.T.Baumbach. A matrix approach to x-ray grazing-incidence diffraction in multilayers. *Z.Phys. B*, 96:341, 1995.